H1–12/94–414

Forward Proportional Chamber Performance in 1994

Zhiqing Zhang*

Laboratoire de l'Accélérateur Linéaire, Bât. 200
CNRS–Université de Paris-Sud, F-91405 Orsay Cedex

Abstract

In order to facilitate the physics analyses, details concerning the forward proportional chamber performance in 1994 are reviewed. Some details of the hardware construction as well as the software convention are also shown such that this note can equally serve as a user guide to the forward proportional chambers.

*ZHANGZQ@FRCPN11.IN2P3.FR

1 Introduction

The forward multiwire proportional chambers (FPC[1])[1] have been constructed basically to provide a fast trigger for the detection of tracks coming from the interaction region in the forward direction along the proton beam direction. Therefore its good performance is important for most of the physics involved and in particular for the heavy flavour physics.

The performance of the FPC especially in terms of its efficiency was not satisfactory during 1993. For the data taking in 1994, due to a better understanding its performance has been improved in some aspects although not yet perfect as we will see in the following.

The hardware construction and the software convention are briefly described in section 2. For more details, refer to Ref.[1] and Appendix of this note. All bad(inefficient) sectors/channels from both signal cables and high voltage(HV) cables are reported in section 3, section 4 describes an efficiency calculation method and shows efficiency results of the FPC. The final section is reserved for discussions and conclusions.

2 Forward proportional chambers (FPC)

The FPC consists of three identical supermodules each being inserted in the forward track detector between the planar drift chamber and the transition radiation detector. Each supermodule consists of two chambers; two wire planes interleaved with four cathode planes. The gap between two adjacent planes is $4\,mm$. The z coordinates of the wire planes can be found in Appendix of this note(Table A1, where two different chamber numbering conventions are also shown). Each wire plane contains a total number of 724 anode wires with a spacing of $2.5\,mm$ between successive wires. Most of the anode wires, made of gold plated tungsten, have a diameter of $30\,\mu m$ with the exception of a few wires at the chamber edges, which have instead a diameter of $50\,\mu m$.

Wires are stung vertically and are connected at one end with a resistor of $1\,M\Omega$ in between. To reduce noise effects and to achieve a constant charge integration time, each wire is further connected to a common ground through a capacitor of $330\,pF$. In order to avoid losing a whole chamber in case one broken wire is present, the wires have been regrouped into 28 sets supplied by 28 HV cables(see Fig.A1 in Appendix). Any two cable connection points on a chamber cover 16 wires except for the first and the last ones which cover instead 10 wires such that there will be either 16 or 10 wires degraded in case of a problem. The HV cable numbering convention can be found in the Appendix.

Ionization of a passing charged particle in the gas[2] is amplified in avalanches around the sense wire. The signals are formed capacitively on cathode pads placed behind a Mylar foil of $100\,\mu$m thickness coated with resistive graphite paint, whose surface resistivity is typically $1\,M\Omega/cm^2$. The whole cathode plane is divided into eight sectors(Fig.A2), and each sector contains 24 ring-shaped pads. Each pad covers an azimuthal angle of either $\pi/8$ for all inner pads or $\pi/16$ for the four outer pads, and is 1.30 to $5.38cm$ wide

[1]FWMWPC or FMWPC is also used.

[2]For technical reasons, the FPC shares the same gas volume as the planar drift chambers. The gas composition is 9.5% Propane, 1.2% Nitrogen, 1% Ethanol, $\sim$ 0.1% Oxygen, and the rest Argon, which is mainly optimized for the planar chambers and that is why the FPC has a different gas than the other proportional chambers(CIP, COP, and BPC).

radially (Table A2). Pads in chamber two are shifted by a half sector in ϕ with respect to those of chamber one (as can be seen from Fig.A2) and by a half pad size in r so that the resolutions on ϕ and r are improved by roughly a factor of two compared with the mechanical pad size and therefore a better noise rejection can be achieved by demanding coincidences between fired pads from different chambers.

The signals collected on pads are read out through strips made of $10\,\mu m$ Cu on $250\,\mu m$ printed circuit board on top of the pad plane with $3.3\,mm$ Nomex in between to the preamplifiers on the chamber ends, which are regrouped there into different signal cables. Each cable reads out 16 pads from either the first 16 pads in a sector(inner sector) of a chamber or the last 8 pads in two corresponding sectors(outer sector) in two adjacent chambers. This gives a total number of 72 signal cables for all three supermodules.

3 HV and noise threshold settings and inefficient channels

One reason for the rather low efficiency in 1993 was thought to be due to the non-optimal HV and noise threshold settings. Therefore, the first thing we did at the beginning of the data taking in 1994 is to re-optimize the settings.

The noise threshold setting in 1993 was $400\,mV$ for all six chambers (1152 pads) except for a few pads with higher threshold. Studies showed that the threshold could be systematically lowered. The final threshold has been set to $250\,mV$ for all six chambers with the exception of the following sectors: $500\,mV(750\,mV)$ for both outer sector 2(3) in chambers 0 and 1, and $500\,mV$ for both outer sector 6 in chambers 4 and 5. The noise contribution can be verified from the online monitoring histograms on level 4, e.g. figure 18704 for the FPC timing, which shows the total number of hits per bunch crossing for a given run. Since the noise contributes randomly, the noise hit pattern should be rather flat compared to the real signals which have been tuned to be peaked in the nominal bunch crossing (number 6(2) for runs taken before(after) June 1, 1994). Fig.1 shows two such distributions for the last two runs taken in 1993 and 1994 respectively. No obvious increase of noise contribution is seen due to the significant modification of the noise thresholds. But there did seem to have been more real signals which arrived one bunch crossing late in 1994 than in 1993. A further look into each bunch crossing as a function of sector shows (Fig.2) no clear sector dependence. In other words it is rather a systematic problem for the whole chambers, and therefore a further tuning will be needed in the future.

The HV setting in 1993 was $1925\,V$ for chambers 0 and 1, and $1950\,V$ for the rest of the chambers. For 1994, we have made an HV scan in 6 points ranging from $1825\,V$ to $1950\,V$. Fig.3 shows the efficiency variation[3] as a function of HV settings. One sees clearly that the plateau behaviour is rather different from one chamber to another. The final setting after a few modifications due to the gas variation was $1840\,V$, $1840\,V$, $1905\,V$, $1820\,V$, $1955\,V$, and $1900\,V$ for chambers 0 through 5 respectively[4].

[3]The efficiencis have been calculated with the method shown in section 4.1.

[4]Careful readers may notice that these HV setting are somewhat low according to Fig.3. This is because the plateau curves were obtained with slightly different(higher) noise thresholds than those

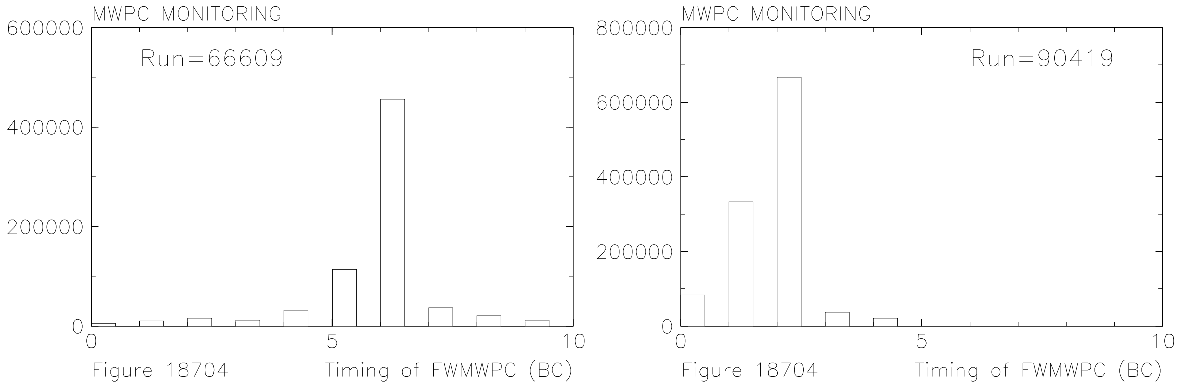

Figure 1: *The FPC timing as shown by one of the online monitoring histograms (figure 18704) for the last two runs (66609 and 90419) in 1993(left) and 1994(right) respectively.*

We have had unfortunately 7 out of 72 cables missing in 1994(Fig.4). They were mainly due to bad connections either at the chamber level(e.g. cable FP0-01-04) or on the cable distribution area(CDA). Most of them are located in chamber 4 in supermodule 2. This is actually the major reason why the overall efficiency for this chamber is particularly low as we will see in section 4.2.

At the beginning of May, two HV cables(FP1-02-12 and FP1-02-13) in chamber 3 were found to be drawing current. Studies showed that this is consistent with a broken wire between these two cables but more likely due to a short circuited capacitor according to the later performance of the chamber. This part was then degraded(Fig.4). The effect(section 4.2) was found to be small due to the flexible HV supply structure mentioned in section 2.

Another problem was the frequent trips occurring on part of the chambers during some of the data taking period, in particular in August. This can be attributed to the gas problem[2].

indicated above.

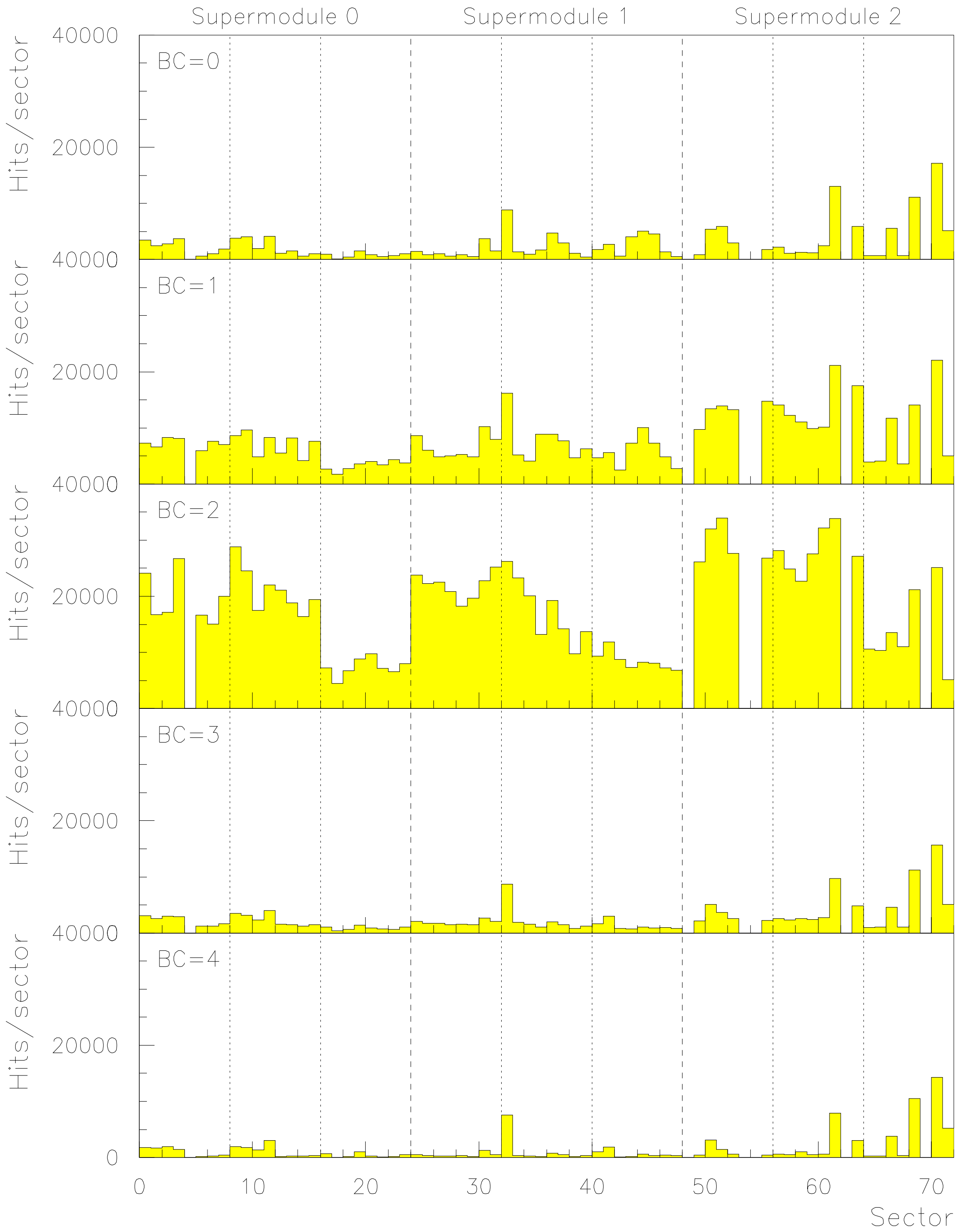

Figure 2: *Number of hits per bunch crossing(BC) and per sector(hardware convention) for run 90008. Five plots from top to bottom are for BC=0, 1, 2, 3, and 4, respectively. The two vertical dashed lines separate three supermodules, each being further separated by two dotted lines into three parts for the inner sectors in chamber 1, the inner sectors in chamber 2, and the outer sectors in chambers 1 and 2.*

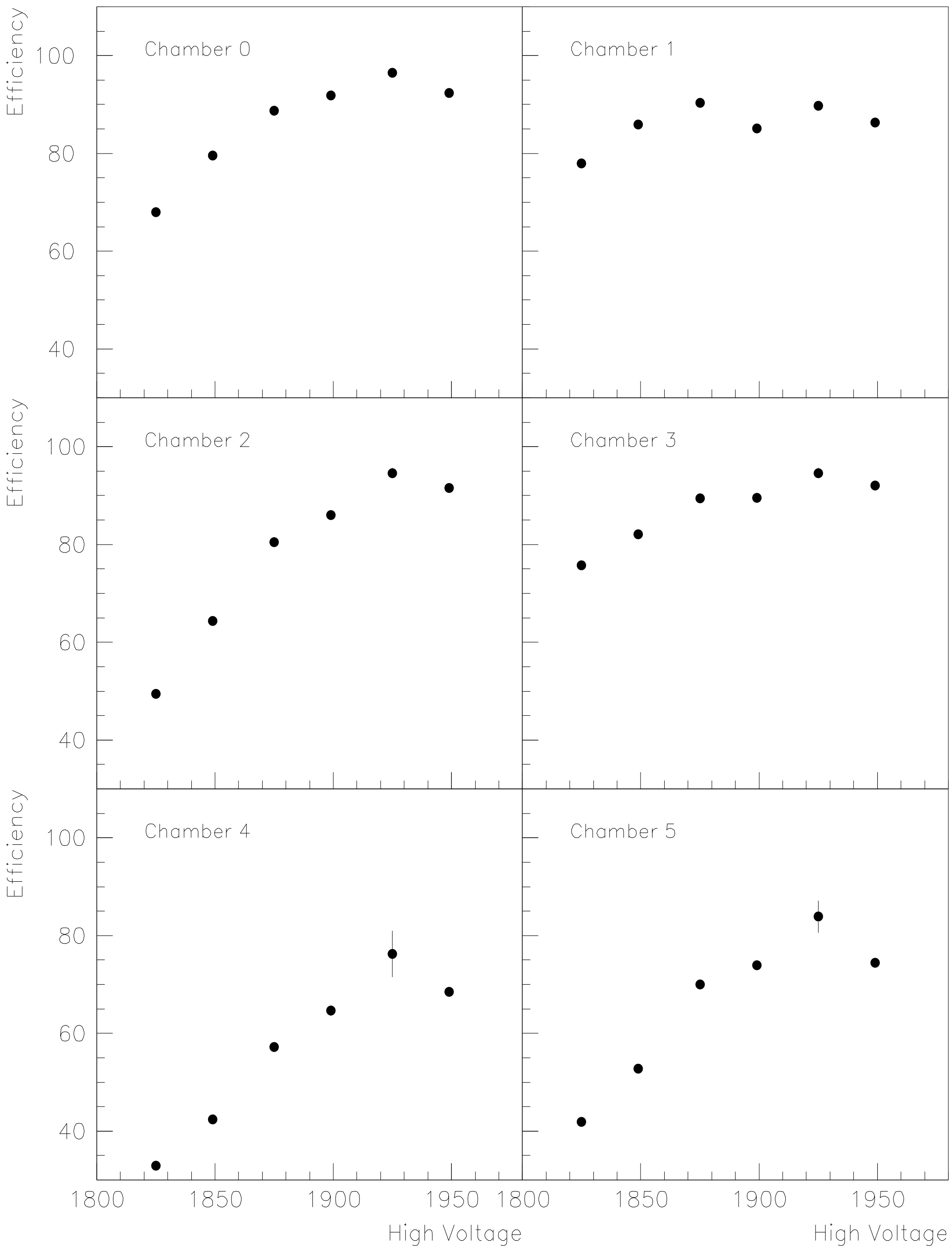

Figure 3: *The FPC efficiency(in %) as a function of the HV settings.*

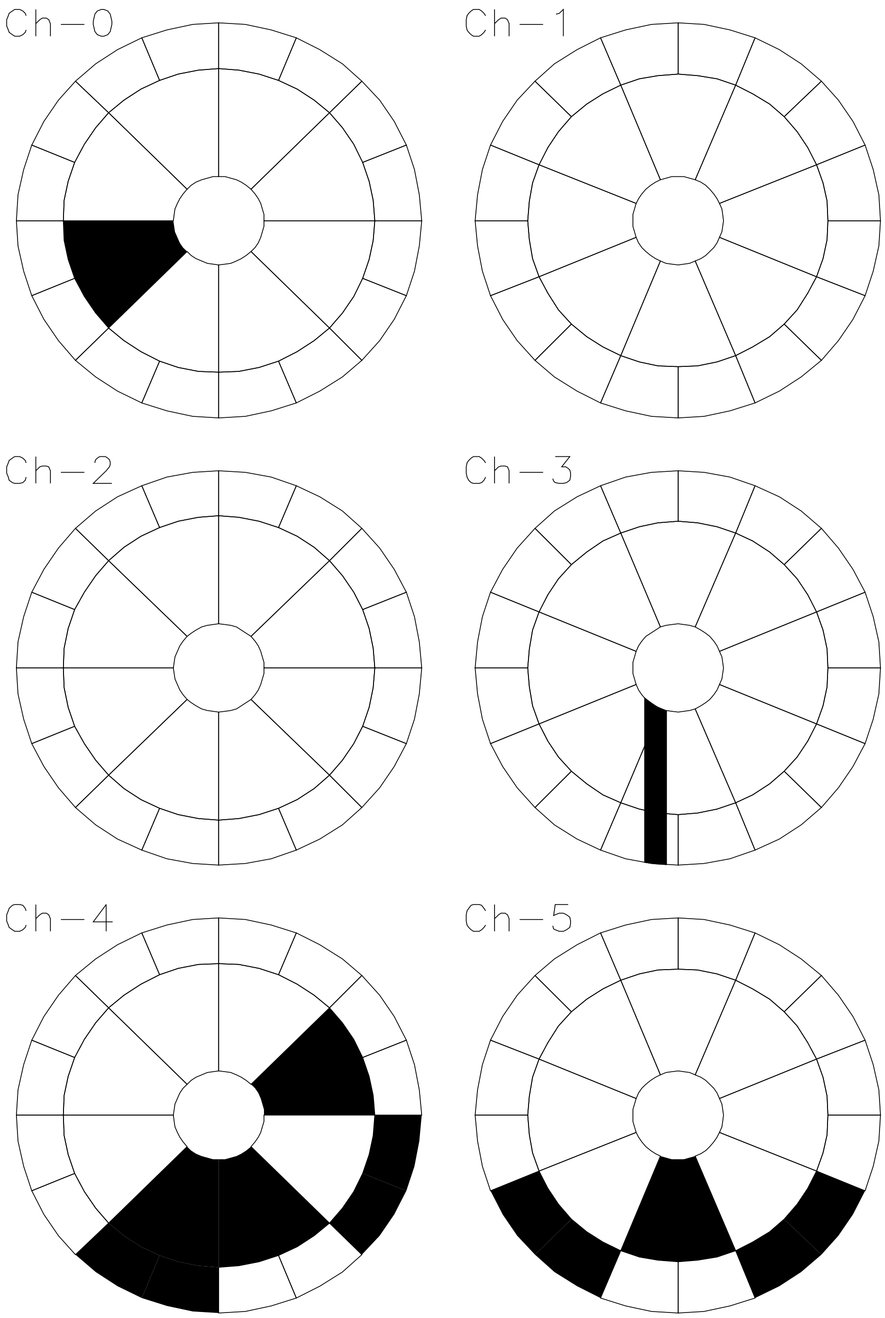

Figure 4: *Inefficient sectors(dark area) in 1994 shown in a view seen in the proton beam direction. The inefficient zone in chamber 3 is due to the degraded HV sector. Note that the four inefficient outer sectors in chambers 4 and 5 are read out by two rather than four signal cables.*

4 FPC efficiency

4.1 Method

Several methods are possible for evaluating the chamber efficiency by using

1. coincidentally fired pads from the FPC alone,
2. forward tracks reconstructed by the planar and radial detectors,
3. a combination of the two.

Each method has its own advantages and disadvantages. The efficiencies to be shown below are calculated based on method (2)[3]. More precisely, only those forward tracks which have at least one planar hit and have a link to the central trackers are selected in order that the calculated efficiency has the least bias from possible fake tracks. The expected impact points of a given track in all chambers through which it passes are determined using the reconstructed track parameters including its curvature. Tracks are further validated by fired pads at the impact points of the tracks in the other chambers than the considered one. If for a given track the considered chamber is in supermodule 1, then both chambers in supermodule 0 are required to be fired for the same track, whereas if the considered chambers is in supermodule 2, then 3 out of 4 chambers should be fired in supermodules 0 and 1. A chamber is defined being efficient if the pad which contains the impact point or any one of its r neighbour is fired. The fired pads are taken only from the nominal bunch crossing.

4.2 Efficiency

Using the methods described in the previous subsection, chamber efficiencies have been calculated for the whole run period in 1994 with an interval ranging from one week for small luminosity runs at the beginning(electron beam runs) to one day for high luminosity runs(positron beam runs). This is shown in Fig.5. For comparison the averaged efficiency values for all runs taken in 1993 are also shown.

A few comments are in order:

- The efficiency is largely improved in 1994 for all the chambers compared to that in 1993, in particular for chambers 2, 4, and 5.
- The relative low overall efficiency(open circle) for chamber 4 is due mainly to the presence of the inefficient sectors as mentioned in section 3 (also in Fig.4) After excluding these inefficient sectors(also for chambers 0 and 5), the resulting efficiency(closed circle) is rather similar to the other chambers (e.g. chamber 5).
- The present understanding of the rather low efficiency in 1993 is due to the non-optimum noise thresholds and HV settings(section 3).
- The efficiency variation is due either to the change in the gas or to the modification of the HV setting.

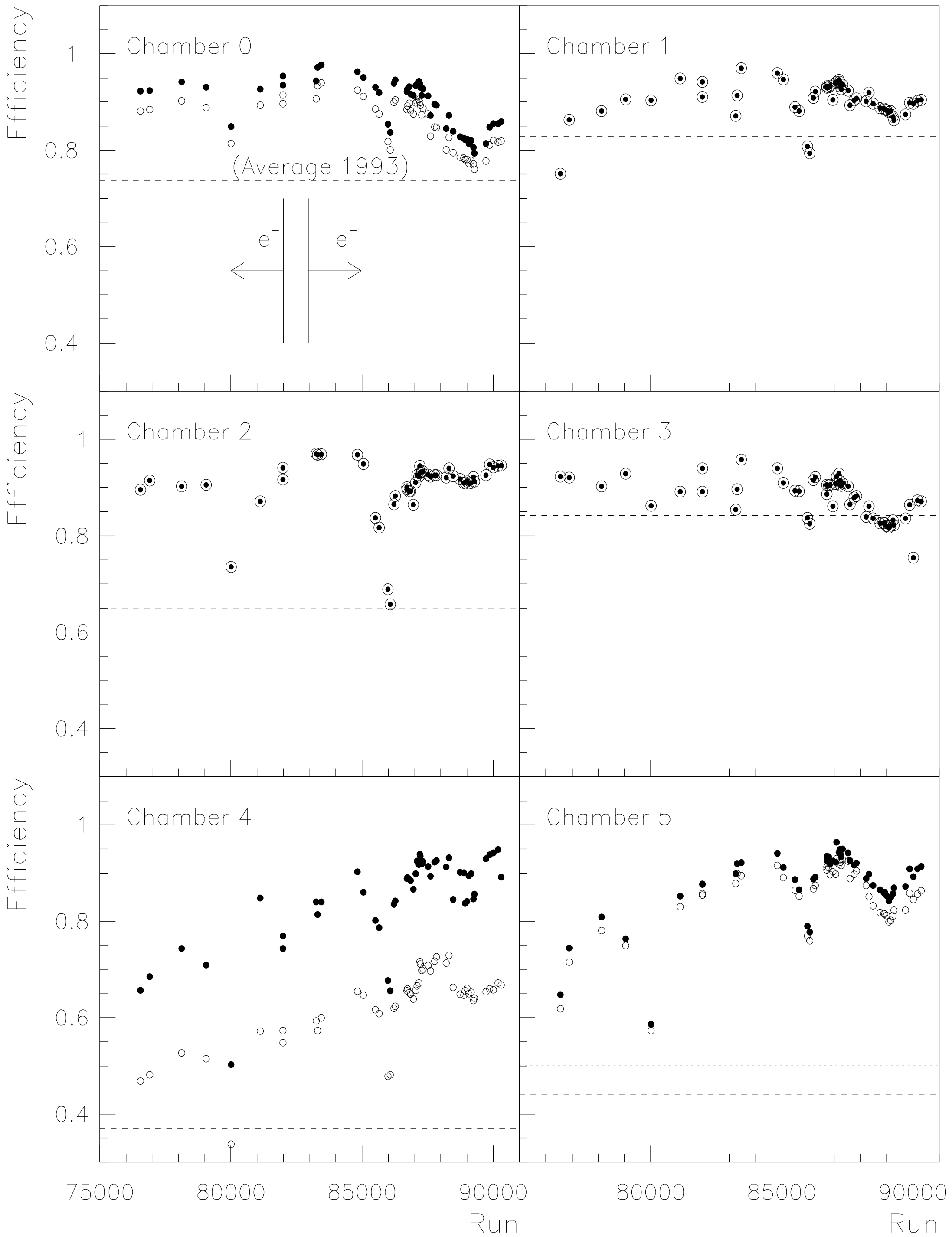

Figure 5: *The FPC efficiency for the whole run period in 1994 compared with the averaged values in 1993. The open circles(dashed lines) show the overall efficiency in 1994(1993), the closed circles(dotted line) the corrected efficiency after excluding the inefficient sectors.*

The efficiencies as a function of pads in the radial direction and in the ϕ direction are shown respectively in Figs. 6 and 7 for a given run(90008). The nonuniformity is due to either the inefficient sectors (Fig.4) or the degraded region in chamber 3 (section 3). Some effects from the spacers (Fig.A2) are also expected. A further reason could be a mechanical defect: the nonuniformity of the gap between the anode wire plane and the cathode pads. The nonuniformity in chamber 1 as shown in Fig.6 may be of this origin. If this is the case then a further tuning on the noise threshold will be needed to compensate for this.

5 Discussions and conclusions

The FPC efficiency has been largely improved in 1994 compared to that in 1993 due to a better understanding of the performance of the chambers and in particular due to re-optimized noise thresholds and high voltage settings. There have also been problems. We have had 7 out of 72 inefficient signal cables owing to the bad connections either on the chamber level or on the CDA, which has to be avoided in the future. We have had one degraded HV zone in chamber 3 which draws current because of a possible broken wire or a short circuited capacitor although the resulting effect on efficiency was small due to the flexible HV supply structure. Some of the chambers suffered from frequent trips during some periods of the data taking, particularly in August where the gas composition varied due to the replacement of a gas filter and the broken gas monitor system[2].

The less stable performance of the FPC compared with the other proportional chambers may be connected to the following three facts although further studies and understanding are needed to draw a firm conclusion: first, the gas used in the FPC, which is the same one as in the planar chambers, is rather different from the other proportinoal chambers, secondly the FPC is located in such a region where it is more sensitive to the beam background conditions, and thirdly the FPC is so large that a local HV plateau behaviour may be present if there is any local nonuniformity of the gap between the anode wire planes and the cathode pads in the same chamber. The latter may be cured by further adjusting the noise thresholds such that different threshold values are allowed in the same chamber.

Acknowledgements

Most of my knowledge on the forward proportional chambers is learnt from A. Courau and S. Mikocki. I would like to acknowledge a lot of helps received from many people during last two years, in particular from J.-C. Bizot, D. Clarke, S. Egli, H. Ehrlichemann, S. Kermiche, G. Lobo, G. Martin-Chassard, K. Mueller, C. Niebuhr, C. Pascaud, and R. Roosen.

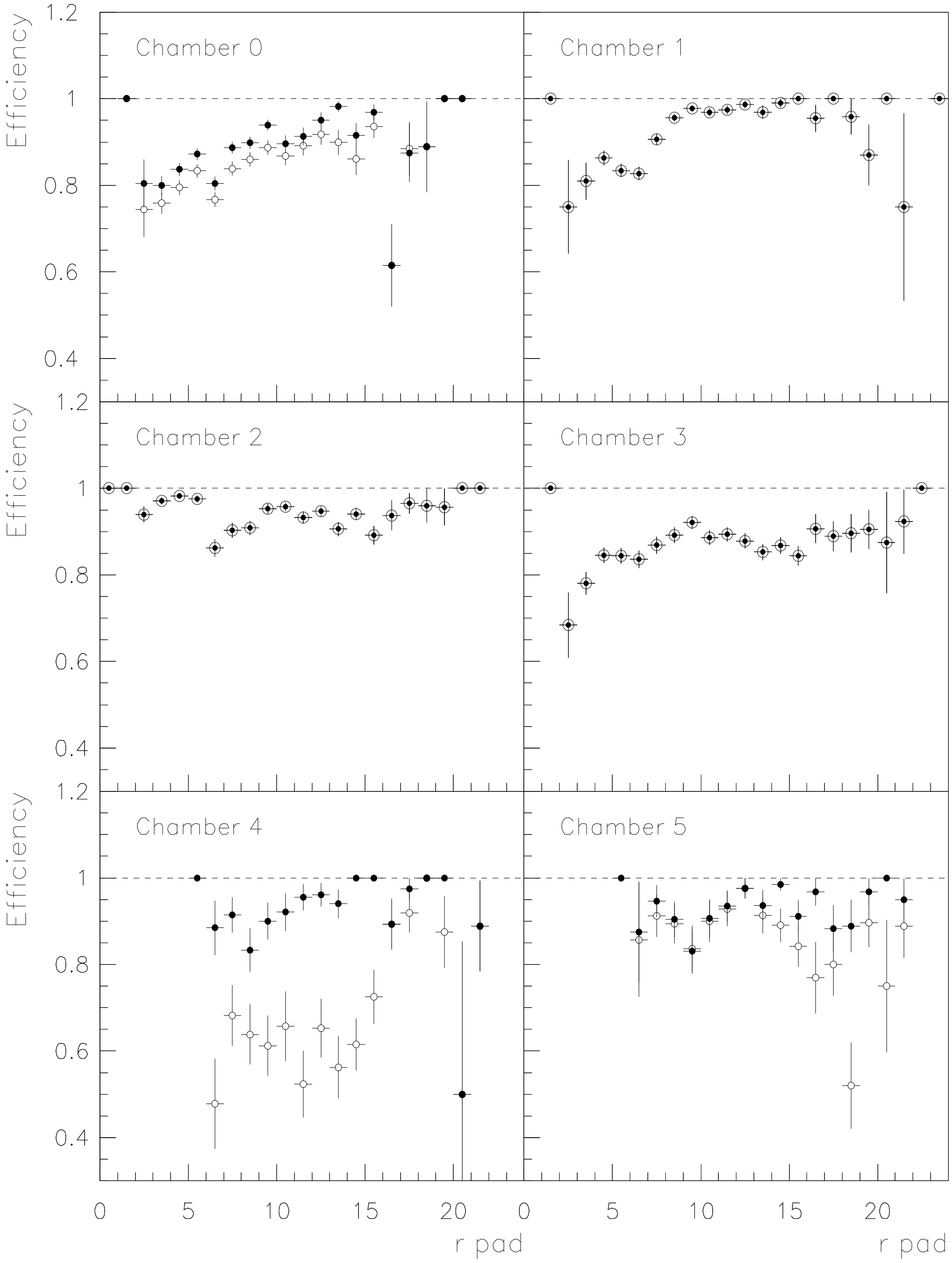

Figure 6: *The FPC efficiency as a function of pads in the radial direction for run 90008. The difference between the upper and lower points in chambers 0, 4 and 5 shows the effect of the inefficient sectors. The missing points at the small radius in last two chambers result from the method in which forward tracks are required to originate from the interaction point.*

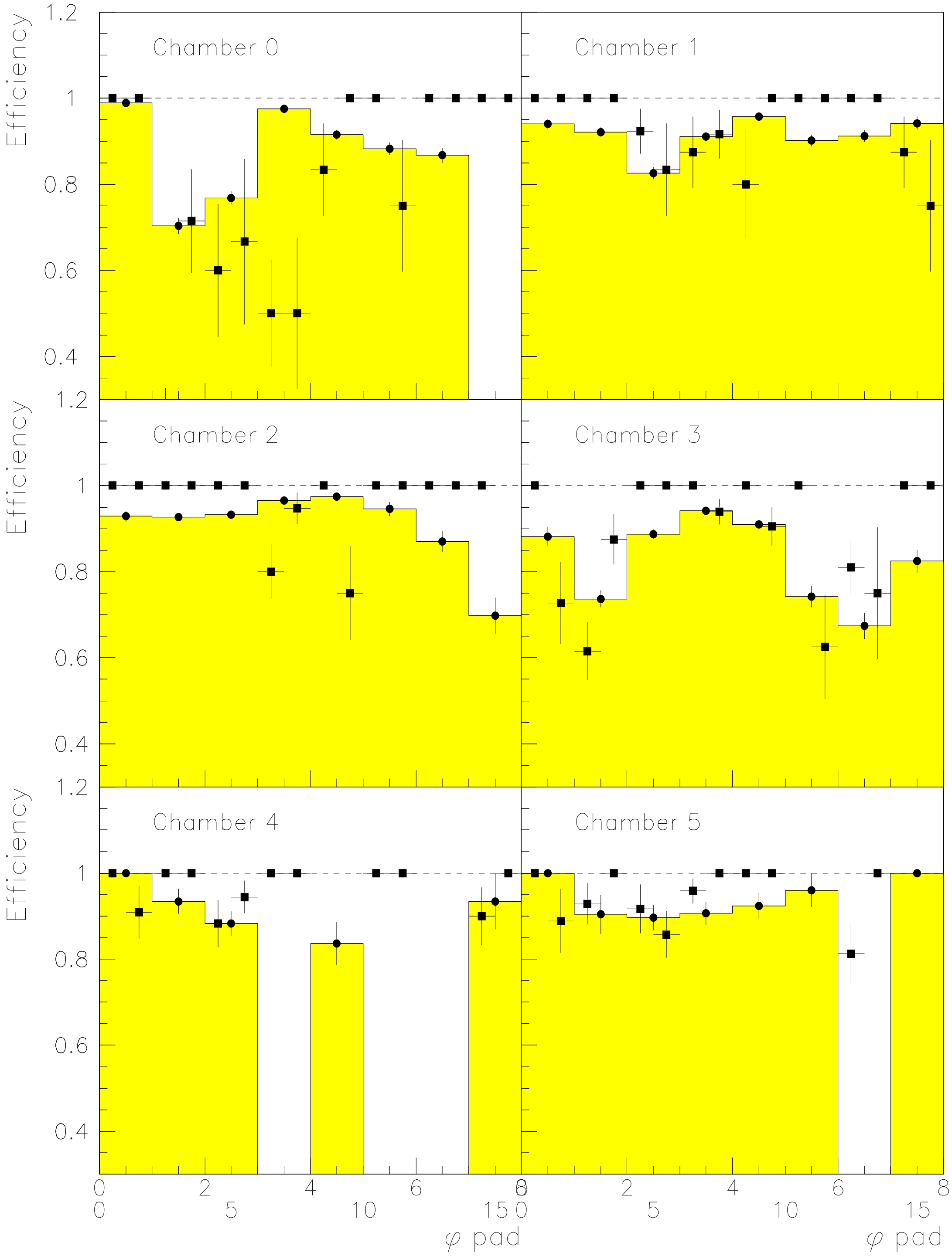

Figure 7: *The FPC efficiency as a function of pads in the ϕ direction for run 90008 showing clearly the effect of the inefficient sectors and the degraded zone. The shaded histogram and the circles are for the 8 inner pads(upper scale) and the squares for the 16 outer ones(lower scale).*

References

[1] H1 Collaboration, "The H1 Detector at HERA", DESY 93-103.

[2] The gas problem as explained by C.Niebuhr was the following: "The first problem occured on July 26, when the ethanol ran out. Later the purifier saturated (around Aug. 24) and was first replaced by a fresh one. A couple of days later it was again replaced by the 'old one' which in the meantime had been regenerated. (A 'fresh' purifier first needs to be saturated with the quenching gas (Propane) until stable conditions are reached, so this time was unnecessary prolonged by replacing it two times). Due to the broken gas chromatograph it took more time than usual to reach again 'normal' gas decomposition."

[3] The efficiency calculation program is taken with only small modifications from a program originally written by S. Egli.

Appendix

The z coordinates of the anode wire and cathode pad planes are shown in Table A1.

Table A1: *The z coordinates of the wire and pad planes of the forward multiwire proportional chamber. Note that two chamber numbering conventions are shown(separated by "/").*

Supermodule	0		1		3	
Chamber	1/0	2/1	1/2	2/3	1/4	2/5
z (cm, wire)	145.1	146.3	187.4	188.6	229.7	230.9
z (cm, pad)	144.7	146.7	187.0	189.0	229.3	231.3

The r coordinates of the cathode pads of chambers one and two are shown in Table A2.

Table A2: *The R coordinates of the cathode pads of chambers one and two.*

	Chamber 1		Chamber 2	
Pad	$r(cm)$	$\Delta r(cm)$	$r(cm)$	$\Delta r(cm)$
0	$16.75 - 18.74$	1.99	$16.75 - 18.05$	1.30
1	$18.74 - 20.20$	1.46	$18.05 - 19.46$	1.40
2	$20.20 - 21.78$	1.57	$19.46 - 20.97$	1.51
3	$21.78 - 23.47$	1.69	$20.97 - 22.61$	1.63
4	$23.47 - 25.30$	1.83	$22.61 - 24.37$	1.76
5	$25.30 - 27.27$	1.97	$24.37 - 26.27$	1.90
6	$27.27 - 29.39$	2.12	$26.27 - 28.31$	2.04
7	$29.39 - 31.68$	2.29	$28.31 - 30.51$	2.20
8	$31.68 - 34.15$	2.47	$30.51 - 32.89$	2.37
9	$34.15 - 36.81$	2.66	$32.89 - 35.45$	2.56
10	$36.81 - 39.67$	2.86	$35.45 - 38.21$	2.76
11	$39.67 - 42.76$	3.09	$38.21 - 41.19$	2.97
12	$42.76 - 46.09$	3.33	$41.19 - 44.39$	3.21
13	$46.09 - 49.68$	3.59	$44.39 - 47.85$	3.46
14	$49.68 - 53.55$	3.87	$47.85 - 51.58$	3.72
15	$53.55 - 57.71$	4.17	$51.58 - 55.60$	4.01
$16 - 17$	$57.71 - 62.21$	4.49	$55.60 - 59.92$	4.32
$18 - 19$	$62.21 - 67.05$	4.84	$59.92 - 64.58$	4.66
$20 - 21$	$67.05 - 72.27$	5.22	$64.58 - 69.61$	5.02
$22 - 23$	$72.27 - 75.00$	2.73	$69.61 - 75.00$	5.38

The HV cables are marked as:

	$FPm - 0n - k$	for **high voltage cables**
with	$m = 0, 1, 2$	stands for supermodule number
	$n = 1, 2$	stands for chamber 1 and 2
	$k = 1, \cdots, 14, 19, \cdots, 32$	stands for numbers in Fig.A1.

Fig.A1 shows a schematic view for the arrangement of the high voltage cables of chambers one and two in any one of the supermodules. Details of 16 wires of cable 19 are also shown. Note that for this particular cable, all but one(the right one as shown in the figure) are short and thin wires($30\,\mu m$), which are fixed on the inner side of the chamber, the right one is a long and big wire($50\,\mu m$), which is not connected on the top in cable 19 but rather connected on the bottom in cable 9. Same is true for cable 14.

The signal cables are numbered in a similar way as for the high voltage cables:

	$FPm - n - 0k$	for **signal cables**
with	$m = 0, 1, 2$	stands for supermodule number
	$n = 01, 02, 12$	stands for chamber 1, chamber 2, chambers 1 and 2
	$k = 0, \cdots, 7$	stands for sector number in each chamber.

This is the hardware convention which is different from the software one, as shown both in Fig.A2.

The high voltage and signal cables are not connected directly to the HV supply system (high voltage distributors) and the signal readout system (receiver cards) in the electronic trailer. Both are rather connected first on the CDA for being able to be disconnected for moving the tracker out of the cryostat as shown schematically in Fig.A3. The details of the cable arrangement on the CDA is shown in Fig.A4 for supermodule 0 (FP0), which is identical to supermodules 1 and 2 (FP1 and FP2).

The high voltage distributor consists of six modules corresponding to six chambers. Fig.A5 shows an example how the HV cables of chamber one in supermodule 0 is arranged in a module.

The signal cables are connected to the receiver cards which are arranged into four modules numbered as crates A7, A8, B4, and B7(located in the MWPC area in the electronic trailer) where the first letter stands for each row running from top to bottom and the second number stands for each column running from left to right. Fig.A6 shows a schematic view of the arrangement of the receiver cards in four crates.

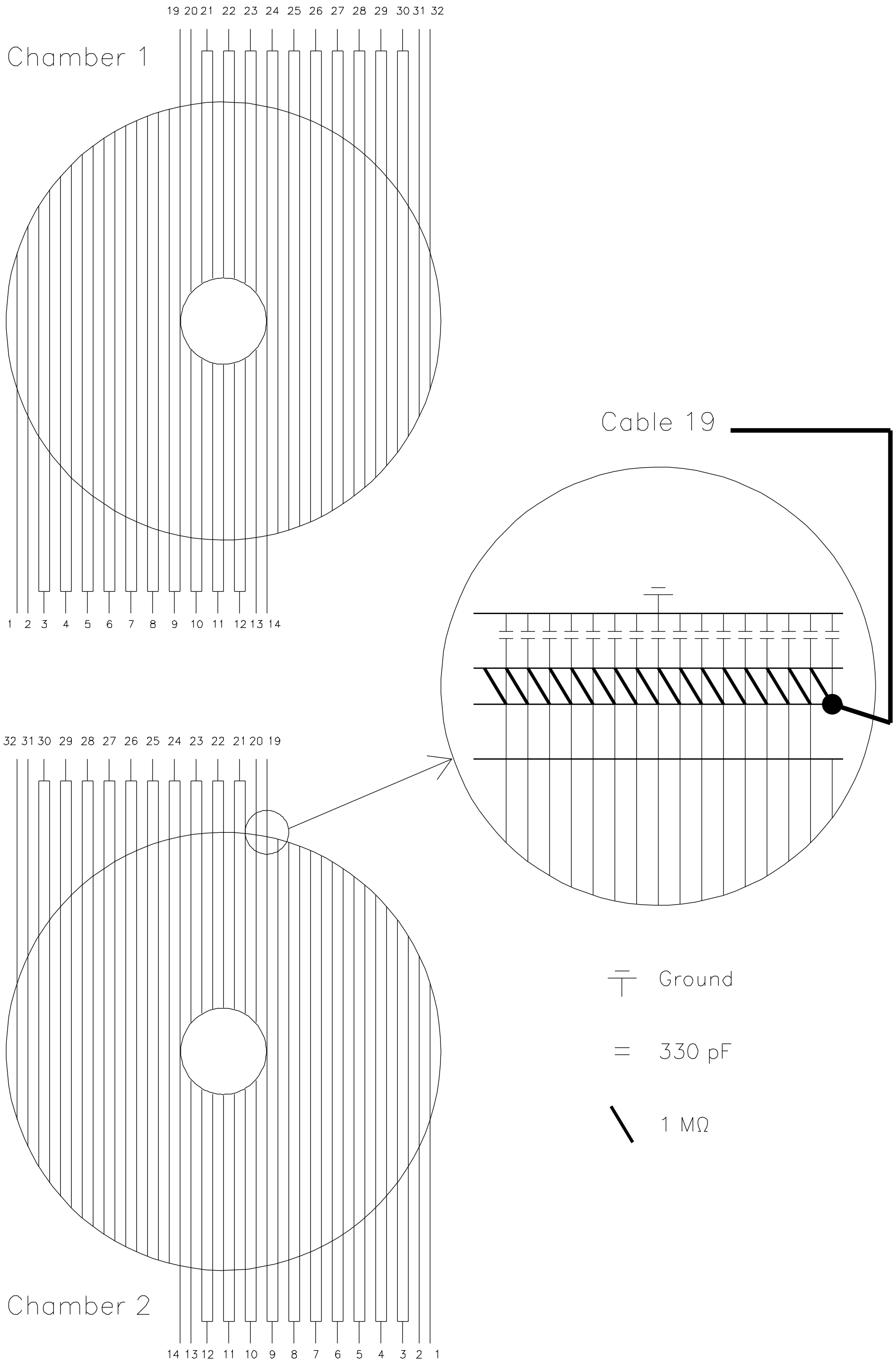

Figure A1: *Transverse view of the wire planes of chamber one (a) and chamber two (b) seen in the proton beam direction direction. The numbers shown stand for the cable numbers. Note that the last wire in cable 19(cable 14) is not connected on the top(bottom) in cable 19(14) but rather connected on the bottom(top) in cable 9(24). For more details, see text.*

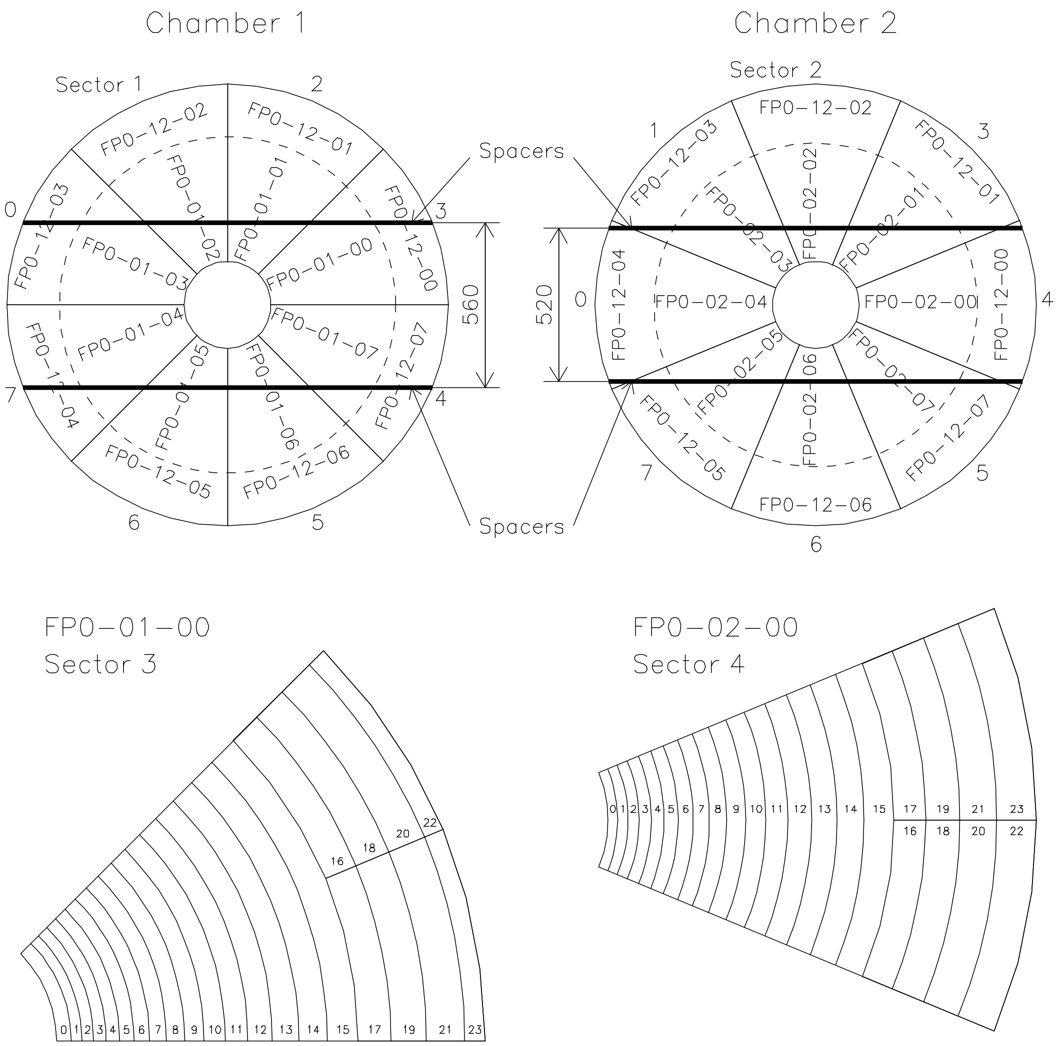

Figure A2: *Transverse view of the cathode pad planes of chamber one (a) and chamber two (b) in supermodule 0 (FP0) seen in the proton beam direction. Two different sector numbering conventions are shown: the hardware one as for the cable numbering (see text) is shown with FP0-01-00 etc within the circles and the software one shown with numbers outside of the circles.*

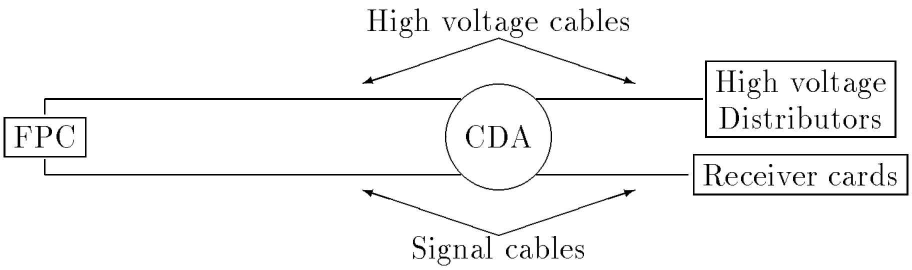

Figure A3: *Schematic view of the high voltage and signal cable connections between the FPC, CDA, and the HV supply system(high voltage distributors) and the signal readout system(receiver cards) in the electronic trailer.*

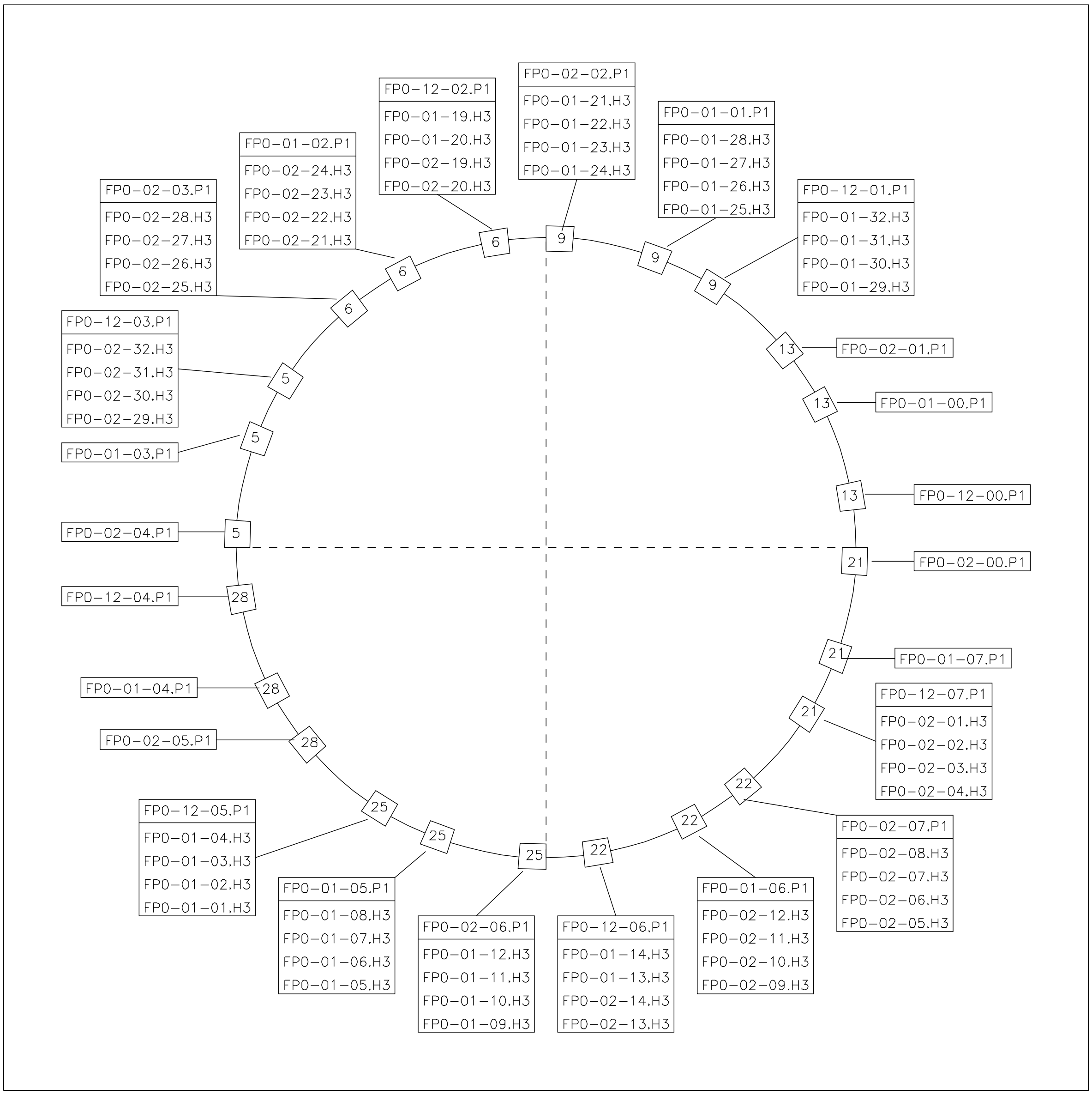

Figure A4: *Details of the high voltage and signal cable connections on CDA seen in the proton beam direction. The numbers along the circle are the slot numbers, signal cables (P1) are shown in the small boxes either alone or on top of the larger ones, in which HV cables (H3) are shown. The other two supermodules (FP1 and FP2) have identical cable arrangements.*

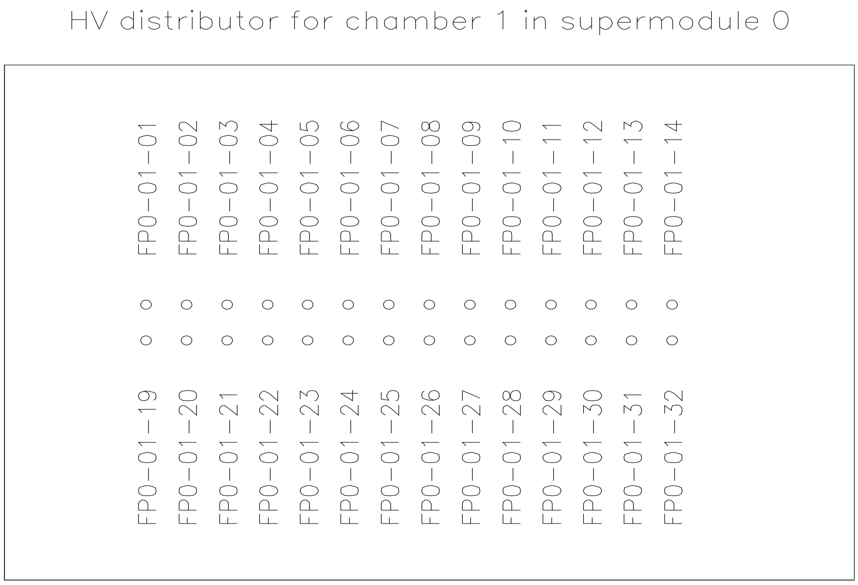

Figure A5: *A schematic view of a high voltage distributor for chamber one in supermodule 0.*

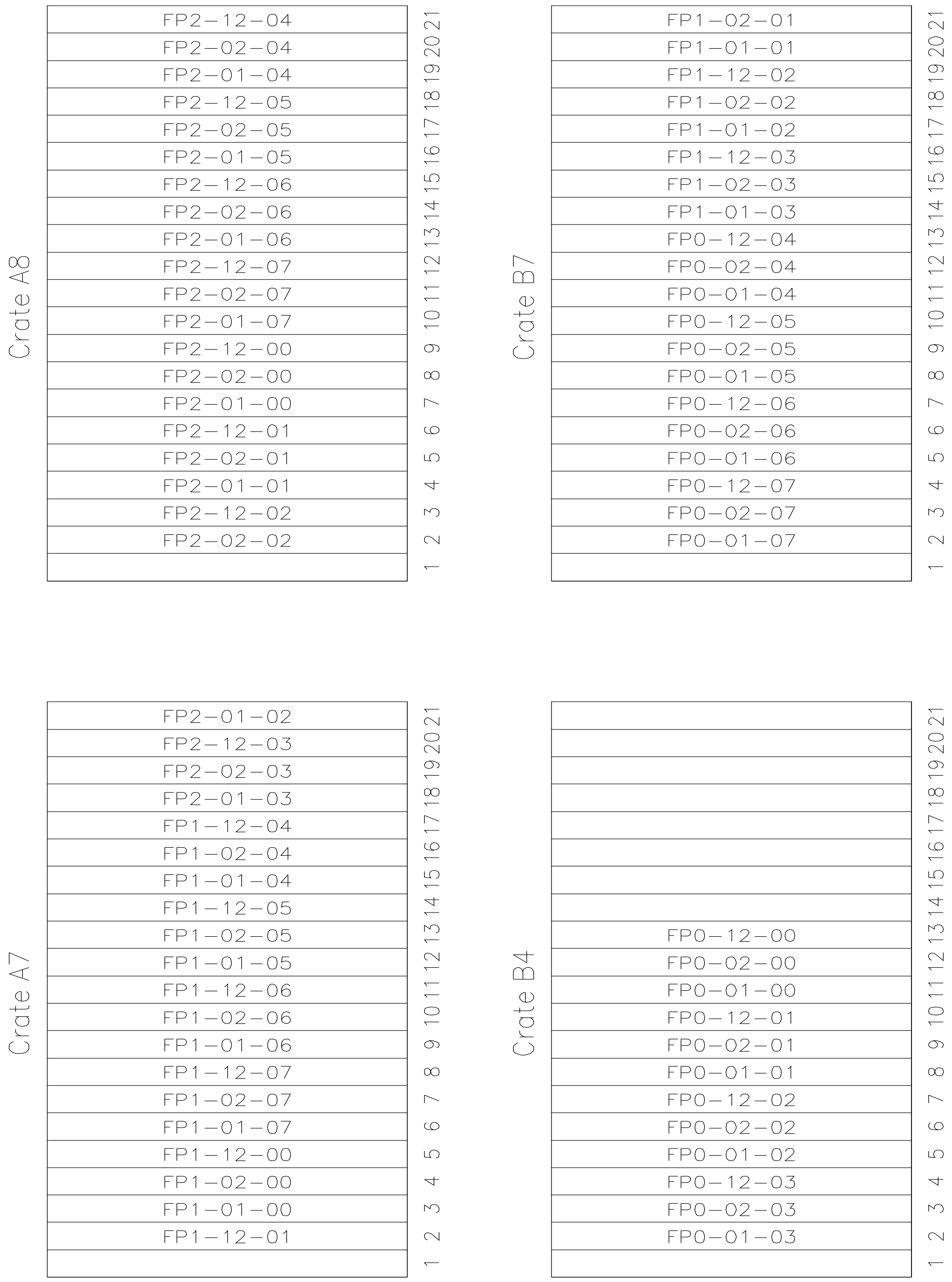

Figure A6: *A schematic view of the arrangement of the receiver cards for the 72 signal cables.*